

# lncRNAs transactivate STAU1-mediated mRNA decay by duplexing with 3' UTRs via Alu elements

Chenguang Gong<sup>1,2</sup> & Lynne E. Maquat<sup>1,2</sup>

Staufen 1 (STAU1)-mediated messenger RNA decay (SMD) involves the degradation of translationally active mRNAs whose 3'-untranslated regions (3' UTRs) bind to STAU1, a protein that binds to double-stranded RNA<sup>1,2</sup>. Earlier studies defined the STAU1-binding site within ADP-ribosylation factor 1 (*ARF1*) mRNA as a 19-base-pair stem with a 100-nucleotide apex<sup>2</sup>. However, we were unable to identify comparable structures in the 3' UTRs of other targets of SMD. Here we show that STAU1-binding sites can be formed by imperfect base-pairing between an Alu element in the 3' UTR of an SMD target and another Alu element in a cytoplasmic, polyadenylated long non-coding RNA (lncRNA). An individual lncRNA can downregulate a subset of SMD targets, and distinct lncRNAs can downregulate the same SMD target. These are previously unappreciated functions of non-coding RNAs and Alu elements<sup>3-5</sup>. Not all mRNAs that contain an Alu element in the 3' UTR are targeted for SMD even in the presence of a complementary lncRNA that targets other mRNAs for SMD. Most known *trans*-acting RNA effectors consist of fewer than 200 nucleotides, and these include small nucleolar RNAs and microRNAs. Our finding that the binding of STAU1 to mRNAs can be transactivated by lncRNAs uncovers an unexpected strategy that cells use to recruit proteins to mRNAs and mediate the decay of these mRNAs. We name these lncRNAs half-STAU1-binding site RNAs (1/2-sbsRNAs).

Using the program mfold<sup>6</sup>, we failed to identify double-stranded RNA (dsRNA) structures similar to the STAU1-binding site (SBS) of *ARF1* mRNA in the 3' UTRs of other SMD targets. This led us to notice that two well-characterized SMD targets—plasminogen activator inhibitor 1 (*SERPINE1*) mRNA and *FLJ21870* mRNA (also known as *ANKRD57* mRNA)<sup>1,2</sup>—contain a single Alu element in their 3' UTRs. We also found that, in three independently performed microarray analyses, ~1.6% of protein-coding transcripts in HeLa cells (human epithelial cells) are upregulated at least 1.8-fold when STAU1 is downregulated<sup>2</sup>, and ~13% of these upregulated transcripts contain a single Alu element in their 3' UTR (Supplementary Table 1). By contrast, only ~4% of HeLa-cell protein-coding transcripts contain one or more Alu elements in their 3' UTR<sup>7</sup>, indicating that 3' UTR Alu elements are enriched in SMD targets relative to the bulk of cellular mRNAs.

Alu elements are the most prominent repeats in the human genome: they constitute more than 10% of the total DNA sequence in a cell and are present at up to 1.4 million copies per cell, and subfamilies of Alu elements share a 300-nucleotide consensus sequence of appreciable similarity<sup>8</sup>. So far, Alu elements have been documented to be *cis* effectors of protein-coding gene expression through their influence on transcription initiation or elongation, alternative splicing, adenosine to inosine (A-to-I) editing or translation initiation<sup>3,5,9</sup>. Because non-coding RNAs (ncRNAs) that base-pair perfectly with mRNA can function in *trans* to generate endogenous short interfering RNAs (siRNAs)<sup>4</sup>, it seemed possible that imperfect base-pairing between the Alu element of a ncRNA and the Alu element of an mRNA 3' UTR could create an SBS, which would regulate mRNA decay. We focused on mRNAs that contain a single 3' UTR Alu element, to avoid the possibility of

intramolecular base-pairing between inverted Alu elements, which could result in A-to-I editing and nuclear retention<sup>10</sup>. Using the Antisense ncRNA Pipeline data set<sup>11,12</sup>, we identified 378 lncRNAs that contain a single Alu element (Supplementary Table 2). Among them, the Alu element of the lncRNA with sequence accession number AF087999 (lncRNA\_AF087999) has the potential to base-pair with the Alu element in the 3' UTR of *SERPINE1* mRNA and *FLJ21870* mRNA (Fig. 1a and Supplementary Fig. 1a) with  $\Delta G$  values of  $-151.7 \text{ kcal mol}^{-1}$  and  $-182.1 \text{ kcal mol}^{-1}$ , respectively (where  $-151.7 \text{ kcal mol}^{-1}$  defined the most stable duplex predicted to form between *SERPINE1* mRNA and any of the 378 lncRNAs) (Supplementary Table 2). This lncRNA, lncRNA\_AF087999, which for reasons that follow is designated 1/2-sbsRNA1, is derived from chromosome 11.

Semiquantitative PCR with reverse transcription (RT-PCR) (Supplementary Fig. 2a) demonstrated that 1/2-sbsRNA1 is present in cytoplasmic HeLa-cell fractions but not nuclear ones and that it is polyadenylated (Supplementary Fig. 2b, c). Downregulating the cellular abundance of the two major isoforms of STAU1 to <10% of normal (see, for example, Fig. 1b) did not affect either the cellular distribution or the abundance of 1/2-sbsRNA1 (Supplementary Fig. 2b). Every human tissue that was examined contained 1/2-sbsRNA1 (Supplementary Fig. 2d), and 1/2-sbsRNA1 is not a substrate for the enzymes dicer 1 (DICER1) or argonaute 2 (AGO2; also known as EIF2C2) (Supplementary Fig. 2e) and thus is distinct from the lncRNAs that generate endogenous siRNAs.

Two forms of 1/2-sbsRNA1 have been reported (NCBI sequence accession numbers AF087999 and AK094046). They differ at their 5' end but have a common Alu element and a common 3' end, which contains a putative polyadenylation signal (AUUAAA) situated 13 nucleotides upstream of a poly(A)<sup>+</sup> tract. RNase protection assays confirmed the presence of one short (S) and one long (L) form of 1/2-sbsRNA1, with different 5' ends and a relative abundance in HeLa cells of 3/1 (Supplementary Fig. 3a). Primer extension (Supplementary Fig. 3b) and semiquantitative RT-PCR (Supplementary Fig. 3c) mapped the 5' end of 1/2-sbsRNA1(S) to a C nucleotide. Therefore, 1/2-sbsRNA1(S) consists of 688 nucleotides, excluding the poly(A)<sup>+</sup> tract (Supplementary Fig. 3d). Whereas some transcripts that are annotated as ncRNAs may be translated<sup>4</sup>, data indicate that 1/2-sbsRNA1(S) is not translated (Supplementary Fig. 4).

Remarkably, in knockdown experiments, not only *STAU1*-directed siRNA but also 1/2-sbsRNA1-directed siRNA increased the levels of *SERPINE1* and *FLJ21870* mRNAs to 2–4.5-fold above normal (Fig. 1b, Supplementary Figs 5 and 6a, and Supplementary Table 3). Furthermore, experiments using the protein-synthesis inhibitor cycloheximide indicated that the 1/2-sbsRNA1-mediated reduction in *SERPINE1* and *FLJ21870* mRNA abundance depends on translation (Supplementary Fig. 6b), as does SMD<sup>13</sup>. The reduction in *SERPINE1* and *FLJ21870* mRNA abundance is attributable to their respective 3' UTR sequences because 1/2-sbsRNA1-directed siRNA also increased the levels of reporter (firefly luciferase, FLUC) mRNAs that contain the appropriate 3' UTR sequence (FLUC-*SERPINE1* 3' UTR and

<sup>1</sup>Department of Biochemistry and Biophysics, School of Medicine and Dentistry, University of Rochester, Rochester, New York 14642, USA. <sup>2</sup>Center for RNA Biology, University of Rochester, Rochester, New York 14642, USA.

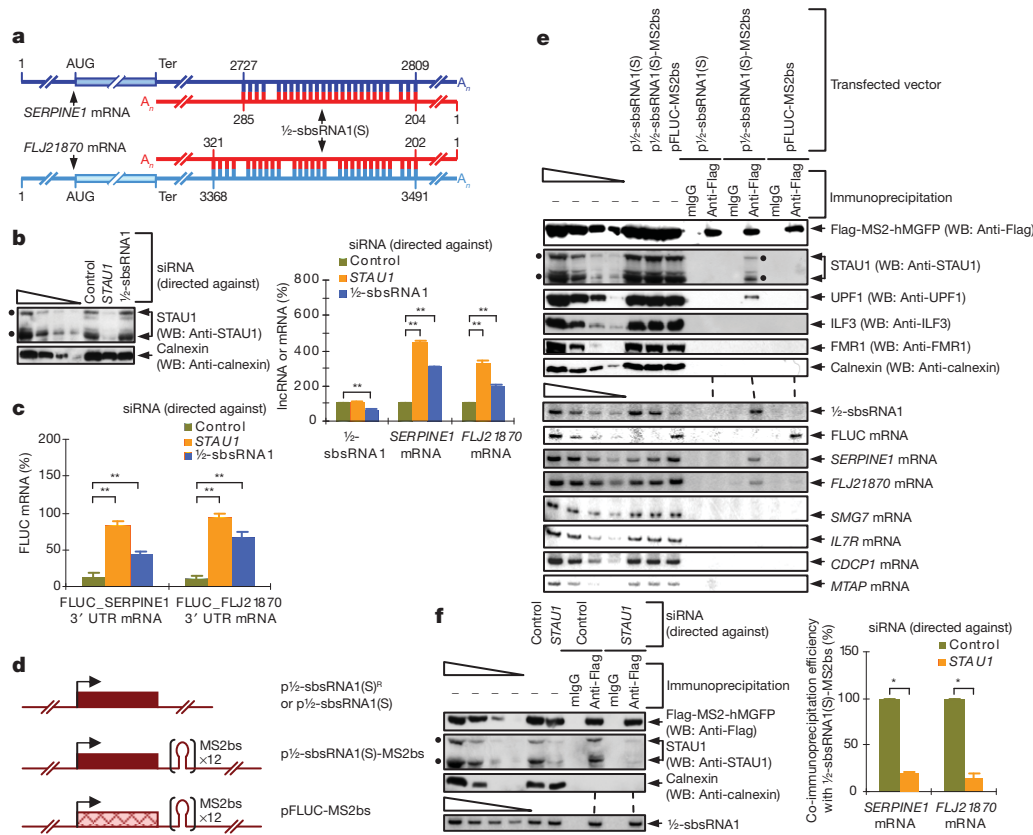


**Figure 1** | 1/2-sbsRNA1 binds to, and reduces the abundance of, specific SMD targets. **a**, Predicted base-pairing between the Alu element in the 3' UTR of *SERPINE1* mRNA or *FLJ21870* mRNA and the Alu element in 1/2-sbsRNA1, where position 1 is defined as the first transcribed nucleotide of each mRNA or of 1/2-sbsRNA1(S). AUG, translation initiation codon; Ter, termination codon. **b**, Left, western blotting (WB), using the antibody designated (as anti-protein name), of lysates of HeLa cells treated with the specified siRNA. Calnexin is a loading control. Right, representation of semiquantitative RT-PCR analyses of 1/2-sbsRNA1, *SERPINE1* mRNA and *FLJ21870* mRNA from the same lysates, where the normalized level of each transcript in the presence of control siRNA is defined as 100. **c**, Representation of semiquantitative RT-PCR analyses of FLUC-*SERPINE1* 3' UTR and FLUC-*FLJ21870* 3' UTR reporter mRNAs in cells that had been transiently transfected with the specified siRNA. For each siRNA, the level of each transcript was normalized to the level of transiently expressed MUP mRNA (from the pCMV-MUP reference plasmid), where the normalized level of FLUC-No SBS mRNA was defined as 100. **d**, Diagrams of expression vectors encoding 1/2-sbsRNA1(S) or 1/2-sbsRNA1(S)<sup>R</sup> (which differs by seven nucleotides, conferring resistance to siRNA), 1/2-sbsRNA1(S)

FLUC-*FLJ21870* 3' UTR mRNAs) relative to a reporter that does not (FLUC-No SBS mRNA) (Fig. 1c, Supplementary Fig. 5 and Supplementary Table 3). The increase in the abundance of *SERPINE1* and *FLJ21870* mRNA that is mediated by 1/2-sbsRNA1-directed siRNA was reversed by co-expression of 1/2-sbsRNA1(S)<sup>R</sup>, which is resistant to the effects of siRNA (Supplementary Fig. 6c), arguing against siRNA-mediated off-target effects. Furthermore, 1/2-sbsRNA1-directed siRNA did not affect the expression of other FLUC reporter mRNAs that contain the 3' UTR of SMD targets that are predicted not to base-pair with 1/2-sbsRNA1 (Supplementary Fig. 7).

If 1/2-sbsRNA1 were to create an SBS by base-pairing with the 3' UTR of *SERPINE1* or *FLJ21870* mRNA, then it should be possible to co-immunoprecipitate complexes of the lncRNA and each mRNA. To test this possibility, lysates of HeLa cells that transiently expressed two plasmid DNAs were immunoprecipitated using anti-Flag antibody: the first plasmid DNA encoded 1/2-sbsRNA1(S)-MS2bs, which contains 12 copies of the MS2 coat-protein binding site (MS2bs)<sup>14</sup>

with 12 copies of MS2bs and FLUC with 12 copies of MS2bs. **e**, Western blotting (top) or semiquantitative RT-PCR (bottom) before (–) or after immunoprecipitation of lysates of formaldehyde-crosslinked HeLa cells that had been transiently transfected with pFlag-MS2-hMGFP and either the denoted 1/2-sbsRNA1(S) expression vector or pFLUC-MS2bs. Immunoprecipitation was performed using either anti-Flag antibody or (as a control for nonspecific immunoprecipitation) mouse immunoglobulin G (mIgG). **f**, As for **e**, except for cells were treated with control or *STAU1*-directed siRNA. Western blotting (top left) and semiquantitative RT-PCR (bottom left, and right), where the co-immunoprecipitation efficiency indicates the level of each mRNA-derived product after immunoprecipitation relative to before immunoprecipitation. Each ratio in the presence of control siRNA is defined as 100%. **b**, **c**, **f**, See Supplementary Fig. 5 for phosphorimages and evaluations of semiquantitative RT-PCR data shown here as histograms. Error bars, s.e.m. \*,  $n = 3$ ,  $P < 0.05$ ; \*\*,  $n = 6$ ,  $P < 0.01$ . **b**, **e**, **f**, Filled circles indicate the two *STAU1* isoforms. Wedges denote threefold dilutions of protein or twofold dilutions of RNA to demonstrate that analyses are semiquantitative, and dashed lines between top and bottom panels align the two panels.

upstream of the lncRNA polyadenylation signal or, as a negative control, 1/2-sbsRNA1(S) or FLUC-MS2bs mRNA (Fig. 1d); and the second plasmid DNA encoded Flag-MS2-hMGFP, which consists of the MS2 coat protein tagged with the polypeptide Flag and fused to monster green fluorescent protein (hMGFP). As expected, before immunoprecipitation, 1/2-sbsRNA1(S), as well as 1/2-sbsRNA1(S)-MS2bs, decreased the abundance of *SERPINE1* and *FLJ21870* mRNA but not other SMD targets that encode the interleukin-7 receptor (IL-7R), CUB-domain-containing protein 1 (CDCP1) or methylthioadenosine phosphorylase (MTAP) (Fig. 1e).

In support of our hypothesis that 1/2-sbsRNA1 creates an SBS with partially complementary mRNA sequences, in lysates of cells expressing 1/2-sbsRNA1(S)-MS2bs, the anti-Flag-antibody-mediated immunoprecipitation of Flag-MS2-hMGFP bound to 1/2-sbsRNA1(S)-MS2bs co-immunoprecipitated endogenous *STAU1* and *SERPINE1* and *FLJ21870* mRNA, as well as UPF1, a factor involved in SMD (Fig. 1e). By contrast, irrelevant proteins, such as calnexin, the dsRNA-binding protein ILF3

(ref. 15), the single-stranded RNA-binding protein FMR1 (ref. 16), and mRNAs that are predicted not to base-pair with 1/2-sbsRNA1, such as those encoding SMG7, IL-7R, CDCP1 and MTAP, were not co-immunoprecipitated (Fig. 1e). *STAU1*-directed siRNA reduced the co-immunoprecipitation of *SERPINE1* mRNA or *FLJ21870* mRNA with 1/2-sbsRNA1(S)-MS2bs to ~19% of normal or ~15% of normal, respectively (Fig. 1f and Supplementary Fig. 5), indicating that STAU1 stabilizes the duplex that is formed between *SERPINE1* or *FLJ21870* mRNA and 1/2-sbsRNA1.

As additional evidence that 1/2-sbsRNA1 creates an SBS by base-pairing with the 3' UTR of *SERPINE1* or *FLJ21870* mRNA, only STAU1 (tagged with the polypeptide HA<sub>3</sub>) but not ILF3 or FMR1 co-immunoprecipitated with 1/2-sbsRNA1 (Supplementary Fig. 8).

To determine whether 1/2-sbsRNA1 is required for the co-immunoprecipitation of STAU1 with *SERPINE1* or *FLJ21870* mRNA, HeLa cells that transiently expressed STAU1-HA<sub>3</sub> and control siRNA or 1/2-sbsRNA1-directed siRNA in the presence or absence of 1/2-sbsRNA1(S)<sup>R</sup> were immunoprecipitated using anti-HA antibodies. Compared with control siRNA, 1/2-sbsRNA1-directed siRNA (which reduced the level of 1/2-sbsRNA1 to ~50% of normal) reduced by about twofold the co-immunoprecipitation of STAU1-HA<sub>3</sub> with *SERPINE1* or *FLJ21870* mRNA (Fig. 2a and Supplementary Fig. 5). By contrast, restoring the level of 1/2-sbsRNA1 to ~100% of normal by expressing 1/2-sbsRNA1-directed siRNA together with 1/2-sbsRNA1(S)<sup>R</sup> restored the co-immunoprecipitation of STAU1-HA<sub>3</sub> with *SERPINE1* or *FLJ21870* mRNA to near normal (Fig. 2a and Supplementary Fig. 5). As expected, the level of *IL7R* mRNA, which binds to STAU1 (ref. 2) but does not contain sequences complementary to 1/2-sbsRNA1, was unaffected by any of these conditions

either before or after immunoprecipitation (Fig. 2a and Supplementary Fig. 5).

We conclude that the SMD of *SERPINE1* and *FLJ21870* mRNA involves base-pairing between their 3' UTR Alu element and the Alu element in 1/2-sbsRNA1. Base-pairing creates an SBS that is stabilized by STAU1. Furthermore, the level of STAU1, and thus the efficiency of SMD, does not alter the level of 1/2-sbsRNA1. Our finding that downregulating *SERPINE1* mRNA to 50% of normal and *FLJ21870* mRNA to 25% of normal failed to detectably decrease the co-immunoprecipitation of STAU1-HA<sub>3</sub> with 1/2-sbsRNA1 (Supplementary Fig. 9) indicates that 1/2-sbsRNA1 may bind to more than just *SERPINE1* and *FLJ21870* mRNAs to recruit STAU1 if not trigger SMD.

The presence of UPF1 in the anti-Flag-antibody-mediated immunoprecipitation of Flag-MS2-hMGFP (Fig. 1e) is consistent with the idea that STAU1 that is bound to a 1/2-sbsRNA1-created SBS associates with UPF1, analogously to how STAU1 that is bound to the *ARF1* mRNA SBS associates with UPF1 (refs 2, 13). Furthermore, downregulating UPF1, like downregulating STAU1, increases the abundance of *SERPINE1* mRNA, *FLJ21870* mRNA and FLUC-*SERPINE1* 3' UTR mRNA by increasing mRNA half-life<sup>1,2</sup>. To test UPF1 function in conjunction with 1/2-sbsRNA1, we analysed the effects of various siRNAs on the production of FLUC-*SERPINE1* 3' UTR mRNA with different versions of the 3' UTR: an intact 3' UTR; a 3' UTR that precisely lacked the region that is partially complementary to 1/2-sbsRNA1 (the binding site (BS) region); and a 3' UTR that contained only this region (Fig. 2b). Relative to control siRNA, *STAU1*-directed siRNA, *UPF1*-directed siRNA or 1/2-sbsRNA1-directed siRNA did not affect the level of FLUC-*SERPINE1* 3' UTR mRNA that lacked the 1/2-sbsRNA1-BS

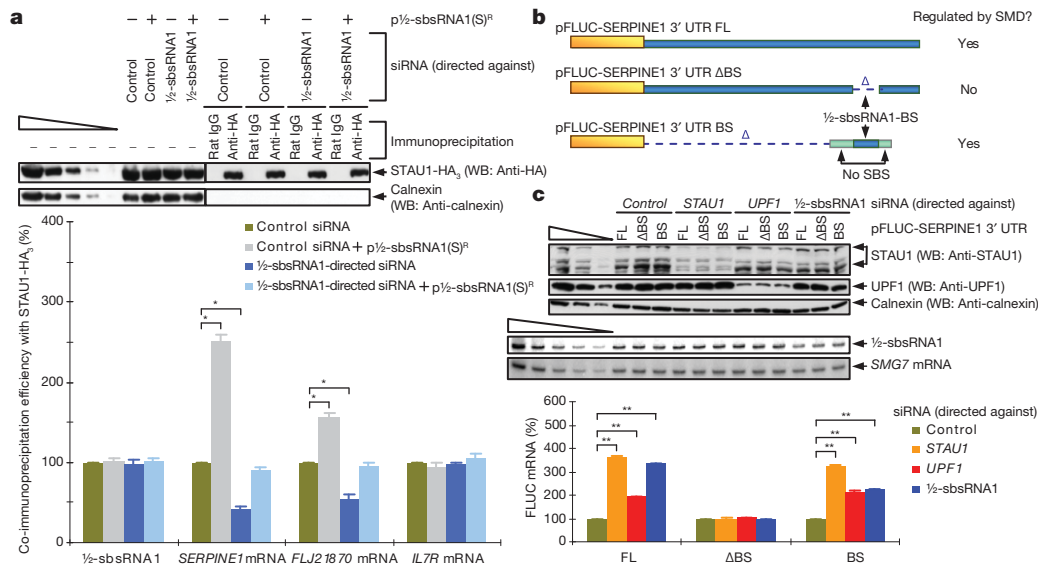


**Figure 2** | 1/2-sbsRNA1 co-immunoprecipitates with STAU1 and is required for STAU1 binding to specific SMD targets. **a**, Western blotting (top) or semiquantitative RT-PCR (bottom) of lysates of formaldehyde-crosslinked HeLa cells that had been transiently transfected with the specified siRNA and either empty vector (-) or p1/2-sbsRNA1(S)<sup>R</sup> (+) before or after immunoprecipitation with anti-HA antibody or rat IgG. After immunoprecipitation, each sample was spiked with *in vitro*-synthesized *Escherichia coli lacZ* mRNA as a loading control. The co-immunoprecipitation efficiency provides the level of each mRNA semiquantitative RT-PCR product after immunoprecipitation relative to before immunoprecipitation, where each ratio in the presence of control siRNA is defined as 100%. **b**, Diagram of pFLUC-*SERPINE1* 3' UTR FL, which contains the full-length (FL) *SERPINE1* 3' UTR, and two 3' UTR deletion variants: pFLUC-*SERPINE1* 3' UTR BS contains only the 1/2-sbsRNA1-binding site (BS), and pFLUC-*SERPINE1* 3' UTR ΔBS contains the entire 3' UTR except for the BS. FLUC sequences are shown in yellow, *SERPINE1* 3' UTR sequences in blue, and the 3' UTR of FLUC-No SBS, which does not bind to STAU1, in green; Δ indicates deleted sequence. The 5'-most green box ensures that ribosomes translating to the FLUC termination codon do not displace STAU1 that has been recruited to the 1/2-sbsRNA1-BS (which is 86 nucleotides, as shown in Supplementary Fig. 1a). **c**, Western blotting (top) and semiquantitative RT-PCR (centre and bottom) of lysates of HeLa cells that had been transiently transfected with the noted pFLUC-*SERPINE1* 3' UTR construct and the pCMV-MUP reference plasmid. Bottom, the normalized level of each FLUC mRNA in the presence of control siRNA is defined as 100%. **a**, **c**, See Supplementary Fig. 5 for phosphorimages and evaluation of semiquantitative RT-PCR data shown here as histograms. **a**-**c**, Error bars, s.e.m. \*,  $n = 3$ ,  $P < 0.05$ ; \*\*,  $n = 6$ ,  $P < 0.01$ .

UTR ΔBS contains the entire 3' UTR except for the BS. FLUC sequences are shown in yellow, *SERPINE1* 3' UTR sequences in blue, and the 3' UTR of FLUC-No SBS, which does not bind to STAU1, in green; Δ indicates deleted sequence. The 5'-most green box ensures that ribosomes translating to the FLUC termination codon do not displace STAU1 that has been recruited to the 1/2-sbsRNA1-BS (which is 86 nucleotides, as shown in Supplementary Fig. 1a). **c**, Western blotting (top) and semiquantitative RT-PCR (centre and bottom) of lysates of HeLa cells that had been transiently transfected with the noted pFLUC-*SERPINE1* 3' UTR construct and the pCMV-MUP reference plasmid. Bottom, the normalized level of each FLUC mRNA in the presence of control siRNA is defined as 100%. **a**, **c**, See Supplementary Fig. 5 for phosphorimages and evaluation of semiquantitative RT-PCR data shown here as histograms. **a**-**c**, Error bars, s.e.m. \*,  $n = 3$ ,  $P < 0.05$ ; \*\*,  $n = 6$ ,  $P < 0.01$ .

(Fig. 2c and Supplementary Fig. 5). However, each of these siRNAs increased the levels of *FLUC-SERPINE1* 3' UTR mRNA and *FLUC* mRNA that contained only the 1/2-sbsRNA1-BS (Fig. 2c and Supplementary Fig. 5). We conclude that, as indicated by its name, 1/2-sbsRNA1 base-pairs with the 3' UTR of *SERPINE1* mRNA and, by analogy, *FLJ21870* mRNA to recruit *STAU1* and its binding partner *UPF1* in a way that triggers a reduction in mRNA abundance. Consistent with previous studies of SMD<sup>2,13</sup>, the *STAU1*- and 1/2-sbsRNA1-mediated reduction in mRNA abundance is due to a decrease in mRNA half-life (Supplementary Fig. 10). With regard to function, scrape-injury repair assays showed that 1/2-sbsRNA1 contributes towards reducing cell migration by targeting *SERPINE1* and *RAB11*-family-interacting protein 1 (*RAB11FIP1*) mRNA for SMD (Supplementary Fig. 11).

Characterizing seven other lncRNAs that contain a single Alu element and consist of <1,000 nucleotides (Supplementary Table 2) confirmed that they too are largely cytoplasmic and polyadenylated (Supplementary Fig. 2b, c and data not shown), and they have the potential to base-pair with the single Alu element in at least one mRNA 3' UTR (Fig. 3a, Supplementary Fig. 1b–d, Supplementary Table 2 and data not shown). Individually downregulating three of these lncRNAs—lncRNA\_BC058830 (1/2-sbsRNA2), lncRNA\_AF075069 (1/2-sbsRNA3) or lncRNA\_BC009800 (1/2-sbsRNA4)—upregulated those tested mRNAs that contain a partially complementary Alu element and are upregulated on *STAU1* or *UPF1* downregulation; downregulation of each lncRNA failed to upregulate mRNAs that lack a partially complementary Alu element (Fig. 3b, Supplementary Fig. 5 and data not shown). Whereas 1/2-sbsRNA2 targeted the 3' UTR Alu

element of *CDCP1* mRNA ( $\Delta G = -153.7 \text{ kcal mol}^{-1}$ ) (Fig. 3b, Supplementary Fig. 5 and Supplementary Table 2), 1/2-sbsRNA3 and 1/2-sbsRNA4 targeted the 3' UTR Alu element of *MTAP* mRNA ( $\Delta G = -203.1$  and  $-264.2 \text{ kcal mol}^{-1}$ , respectively) (Fig. 3b, Supplementary Fig. 5 and Supplementary Table 2). Furthermore, none of the three lncRNAs downregulated *SERPINE1* mRNA ( $\Delta G = 0$ ,  $-66.4$  and  $-108.2 \text{ kcal mol}^{-1}$  for 1/2-sbsRNA2, 1/2-sbsRNA3 and 1/2-sbsRNA4, respectively) (Fig. 3b, Supplementary Fig. 5 and Supplementary Table 2), but two of them downregulated *FLJ21870* mRNA about twofold ( $\Delta G = -261.9$  and  $-444.2 \text{ kcal mol}^{-1}$  for 1/2-sbsRNA3 and 1/2-sbsRNA4, respectively) (Fig. 3b, Supplementary Fig. 5 and Supplementary Table 2).

These findings illustrate the potentially complex network of regulatory events that are controlled by lncRNA–mRNA duplexes that bind to *STAU1*, a network that is reminiscent of the web of regulatory mechanisms that are mediated by microRNAs<sup>17</sup>. Notably, both *CDCP1* mRNA and *MTAP* mRNA were upregulated at least twofold on *STAU1* downregulation in experiments reported here (Fig. 3b), and indeed *CDCP1* mRNA is among those mRNAs that were upregulated minimally (1.8 fold) on *STAU1* downregulation<sup>2</sup> (Supplementary Table 1). However, because *MTAP* mRNA was upregulated only  $\sim 1.5$  fold<sup>2</sup>, it is not included in Supplementary Table 1. Thus, Supplementary Table 1 must be considered to provide only a partial list of mRNAs that are modulated by one or more 1/2-sbsRNAs. Conceivably, the degree of modulation could vary in different cell types (Supplementary Fig. 2d) or developmental stages depending on the abundance of the 1/2-sbsRNA(S) and on proteins that inhibit or enhance base-pairing.

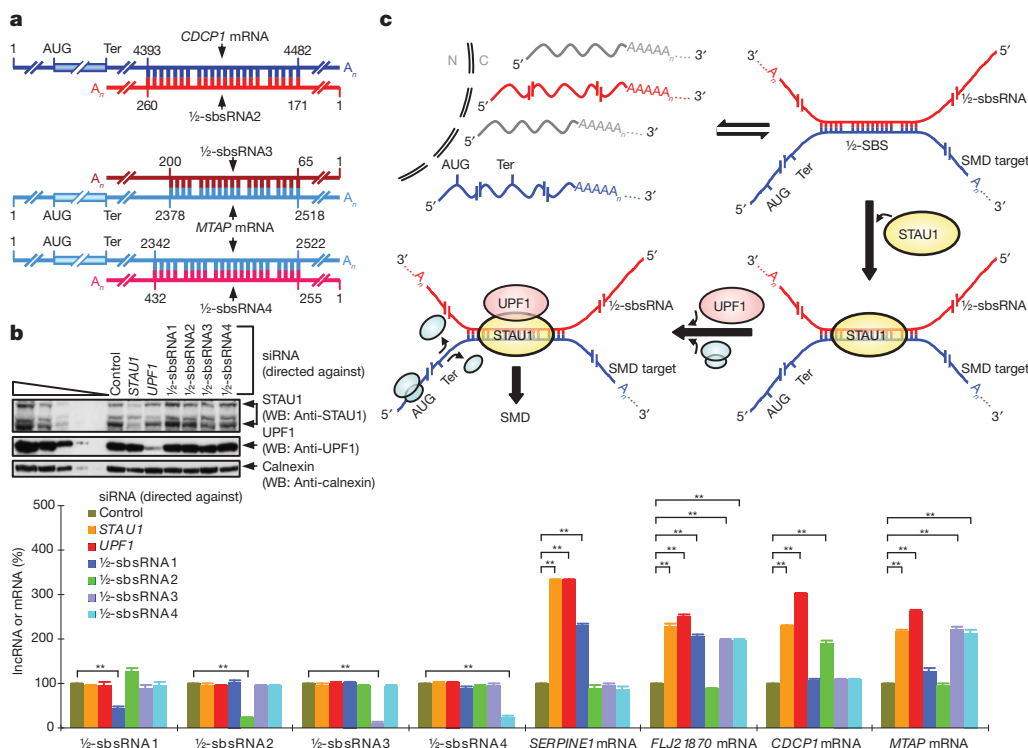


**Figure 3 | Evidence that 1/2-sbsRNA2, 1/2-sbsRNA3 and 1/2-sbsRNA4 base-pair with particular mRNA 3' UTRs and decrease mRNA abundance, as do *STAU1* and *UPF1*.** **a**, Predicted base-pairing between the 3' UTR Alu element of *CDCP1* mRNA (NCBI Nucleotide accession number NM\_022842) and 1/2-sbsRNA2, or *MTAP* mRNA (accession number NM\_002451) and 1/2-sbsRNA3 as well as 1/2-sbsRNA4, where position 1 is defined as the first nucleotide listed in the NCBI Nucleotide database for each mRNA or lncRNA. **b**, Essentially as in Fig. 1b. See Supplementary Fig. 5 for phosphorimages and evaluation of semiquantitative RT-PCR data shown here as histograms. Error bars, s.e.m. \*\*,  $n = 6$ ,  $P < 0.01$ . **c**, Model for how an Alu-element-containing

1/2-sbsRNA that is polyadenylated and largely cytoplasmic (red) base-pairs with a partially complementary Alu element, that is, a half-*STAU1* binding site (1/2-SBS), within the 3' UTR of a particular mRNA (blue) to trigger SMD. Base-pairing forms a functional SBS. The *STAU1*-bound SBS triggers SMD in a *UPF1*-dependent mechanism when translation terminates sufficiently upstream of the SBS so that translating ribosomes (blue ovals) do not remove bound *STAU1*. The 1/2-sbsRNA is not destroyed in the process. C, cytoplasm; N, nucleus; Ter, termination codon (which is generally, but not necessarily, a normal termination codon).

It is important to note that  $\Delta G$  values are not in themselves absolute predictors of SBS function. For example, although 1/2-sbsRNA2 is predicted to base-pair with the 3' UTR Alu element of BAG5 mRNA (with  $\Delta G = -416 \text{ kcal mol}^{-1}$ ), BAG5 mRNA is not targeted for SMD in HeLa cells (Supplementary Fig. 12). The 3' UTR Alu element of BAG5 mRNA may be physically inaccessible to base-pairing with 1/2-sbsRNA2. Nevertheless, base-pairing itself may not be sufficient for SBS function because converting the 100-nucleotide apex of the intramolecular ARF1 mRNA SBS to a 4-nucleotide loop that is predicted not to disrupt the adjacent 19-base-pair stem of the ARF1 mRNA SBS reduces STAU1 binding *in vivo* by 50% (ref. 2).

Here we report an unforeseen role for some of the lncRNAs that contain Alu elements: the creation of SBSs by intermolecular base-pairing with an Alu element in the 3' UTR of one or more mRNAs. We conclude that SBSs can form either through intramolecular base-pairing, as exemplified by the ARF1 mRNA SBS, or intermolecular base-pairing between a 1/2-SBS in an mRNA 3' UTR and a complementary 1/2-sbsRNA in the form of a largely cytoplasmic lncRNA (Fig. 3c).

There are estimated to be tens of thousands of human ncRNAs that have little or no ability to direct protein synthesis and that are distinct from ribosomal RNAs, transfer RNAs, small nuclear RNAs, small nucleolar RNAs, siRNAs and microRNAs<sup>18</sup>. Thus, the model in which partially complementary ncRNA–mRNA duplexes can form SBSs may extend to the creation of binding sites for other dsRNA-binding proteins. Because only 23% of lncRNAs were found to contain one or more Alu elements, it is also possible that lncRNA–mRNA duplexes that do not involve Alu elements could increase the number of ncRNAs that regulate gene expression by SMD or a different dsRNA-binding-protein-dependent pathway.

## METHODS SUMMARY

A Perl program, Alu\_Mask, was written and used together with the program RepeatMasker (<http://www.repeatmasker.org/cgi-bin/WEBRepeatMasker>) to define Alu elements. A Perl program, RNA\_RNA\_anneal, which uses a recursive algorithm<sup>19,20</sup>, was generated to predict intermolecular duplexes between Alu elements in lncRNAs and proven or putative SMD targets. Duplexes were then validated using the program RNAstructure 4.6 (<http://rna.urmc.rochester.edu/RNAstructure.html>), which provides folding free energy changes ( $\Delta G$ ). Human cells (HeLa or HaCaT) were transiently transfected with the specified plasmids or siRNAs as previously described<sup>1</sup>. For mRNA half-life measurements, Tet-Off HeLa cells (Clontech) were used. If the cells had been crosslinked with formaldehyde, cells were sonicated six times for 30 s to facilitate lysis, and crosslinks were reversed by heating at 65 °C for 45 min after immunoprecipitation. Immunoprecipitation was performed as previously described<sup>1</sup>. Protein was purified, and western blotting was performed as previously described<sup>1</sup>. RNA was purified from total, nuclear or cytoplasmic cell fractions or immunoprecipitated from total-cell lysates as previously reported<sup>1</sup>. Poly(A)<sup>+</sup> RNA was extracted from total-cell RNA by using the Oligotex mRNA Mini Kit (Qiagen). Semiquantitative RT–PCR and quantitative real-time RT–PCR were carried out as previously described<sup>1</sup>, except in certain cases in which RT was primed using oligo(dT)<sub>18</sub> rather than random hexamers. For RNase protection assays, the RPA III Ribonuclease Protection Assay Kit (Ambion) was used, together with uniformly labelled RNA probes that were generated by transcribing linearized pcDNA3.1/Zeo(+)\_Chr11\_66193000–66191383 (which contains 1/2-sbsRNA1(S) and upstream and downstream flanking sequences) *in vitro* using [ $\alpha$ -<sup>32</sup>P]UTP (PerkinElmer) and the MAXIscript T7 Kit (Ambion). Cells were visualized using an Eclipse TE2000-U inverted fluorescence microscope (Nikon), and a 480-nm excitation wavelength was used for phase contrast microscopy. Images were captured using TILLvisiON software (TILL Photonics). Scrape-injury repair assays were performed essentially as previously published<sup>21,22</sup>. All data were derived from at least three independently performed experiments that did not vary by more than the amount shown, and *P* values for all semiquantitative RT–PCR results were <0.05. All *P* values were determined by one-tailed *t*-tests.

**Full Methods** and any associated references are available in the online version of the paper at [www.nature.com/nature](http://www.nature.com/nature).

**Received 20 June; accepted 25 November 2010.**

- Gong, C., Kim, Y. K., Woeller, C. F., Tang, Y. & Maquat, L. E. SMD and NMD are competitive pathways that contribute to myogenesis: effects on PAX3 and myogenin mRNAs. *Genes Dev.* **23**, 54–66 (2009).
- Kim, Y. K. *et al.* Staufen1 regulates diverse classes of mammalian transcripts. *EMBO J.* **26**, 2670–2681 (2007).
- Cordaux, R. & Batzer, M. A. The impact of retrotransposons on human genome evolution. *Nature Rev. Genet.* **10**, 691–703 (2009).
- Wilusz, J. E., Sunwoo, H. & Spector, D. L. Long noncoding RNAs: functional surprises from the RNA world. *Genes Dev.* **23**, 1494–1504 (2009).
- Walters, R. D., Kugel, J. F. & Goodrich, J. A. InvAluable junk: the cellular impact and function of Alu and B2 RNAs. *IUBMB Life* **61**, 831–837 (2009).
- Zuker, M. Mfold web server for nucleic acid folding and hybridization prediction. *Nucleic Acids Res.* **31**, 3406–3415 (2003).
- Yulug, I. G., Yulug, A. & Fisher, E. M. The frequency and position of Alu repeats in cDNAs, as determined by database searching. *Genomics* **27**, 544–548 (1995).
- Batzer, M. A. & Deininger, P. L. Alu repeats and human genomic diversity. *Nature Rev. Genet.* **3**, 370–379 (2002).
- Hasler, J. & Strub, K. Alu elements as regulators of gene expression. *Nucleic Acids Res.* **34**, 5491–5497 (2006).
- Chen, L. L., DeCervo, J. N. & Carmichael, G. G. Alu element-mediated gene silencing. *EMBO J.* **27**, 1694–1705 (2008).
- Pang, K. C. *et al.* RNAdb 2.0—an expanded database of mammalian non-coding RNAs. *Nucleic Acids Res.* **35**, D178–D182 (2007).
- Engström, P. G. *et al.* Complex loci in human and mouse genomes. *PLoS Genet.* **2**, e47 (2006).
- Kim, Y. K., Furic, L., Desgroseillers, L. & Maquat, L. E. Mammalian Staufen1 recruits Upf1 to specific mRNA 3'UTRs so as to elicit mRNA decay. *Cell* **120**, 195–208 (2005).
- Kim, H. H. *et al.* HuR recruits let-7/RISC to repress c-Myc expression. *Genes Dev.* **23**, 1743–1748 (2009).
- Kuwano, Y. *et al.* NF90 selectively represses the translation of target mRNAs bearing an AU-rich signature motif. *Nucleic Acids Res.* **38**, 225–238 (2010).
- Ashley, C. T. Jr, Wilkinson, K. D., Reines, D. & Warren, S. T. FMR1 protein: conserved RNP family domains and selective RNA binding. *Science* **262**, 563–566 (1993).
- Bartel, D. P. MicroRNAs: target recognition and regulatory functions. *Cell* **136**, 215–233 (2009).
- Kapranov, P., Willingham, A. T. & Gingeras, T. R. Genome-wide transcription and the implications for genomic organization. *Nature Rev. Genet.* **8**, 413–423 (2007).
- Mathews, D. H., Sabina, J., Zuker, M. & Turner, D. H. Expanded sequence dependence of thermodynamic parameters improves prediction of RNA secondary structure. *J. Mol. Biol.* **288**, 911–940 (1999).
- Xia, T. *et al.* Thermodynamic parameters for an expanded nearest-neighbor model for formation of RNA duplexes with Watson–Crick base pairs. *Biochemistry* **37**, 14719–14735 (1998).
- Liang, C. C., Park, A. Y. & Guan, J. L. *In vitro* scratch assay: a convenient and inexpensive method for analysis of cell migration *in vitro*. *Nature Protocols* **2**, 329–333 (2007).
- Providence, K. M. *et al.* SERPINE1 (PAI-1) is deposited into keratinocyte migration ‘trails’ and required for optimal monolayer wound repair. *Arch. Dermatol. Res.* **300**, 303–310 (2008).

**Supplementary Information** is linked to the online version of the paper at [www.nature.com/nature](http://www.nature.com/nature).

**Acknowledgements** We thank D. Mathews and A. Grossfield for the use of computer clusters, D. Mathews for access to the program Structure 5.0, K. Nerhrke for fluorescence microscope time, S. de Lucas and J. Ortiz for anti-STAU1 antibodies, M. Gorospe for pcDNA3-MS2bsX12, S. Higgins and P. Higgins for HaCaT cells and advice on the scrape-injury repair assay, J. Wang for the initial BAG5 mRNA assays, and O. Isken, M. Gleghorn and D. Mathews for comments on the manuscript. This work was supported by the National Institutes of Health (GM074593 to L.E.M.) and an Elon Huntington Hooker Graduate Student Fellowship (C.G.).

**Author Contributions** C.G. wrote the Perl programs and performed the bioinformatics analyses and wet-bench experiments. C.G. and L.E.M. analysed the computational data, designed the wet-bench experiments, analysed the resultant data and wrote the manuscript.

**Author Information** Reprints and permissions information is available at [www.nature.com/reprints](http://www.nature.com/reprints). The authors declare no competing financial interests. Readers are welcome to comment on the online version of this article at [www.nature.com/nature](http://www.nature.com/nature). Correspondence and requests for materials should be addressed to L.E.M. ([lynnemaquat@urmc.rochester.edu](mailto:lynnemaquat@urmc.rochester.edu)).

## METHODS

**Computational analyses.** A Perl program, *Alu\_Mask*, was designed to define Alu elements within known and putative SMD targets and ncRNAs, on the basis of results obtained using the program RepeatMasker (<http://www.repeatmasker.org/cgi-bin/WEBRepeatMasker>).

A Perl program, *RNA\_RNA\_anneal*, was developed to predict Alu-element base-pairing between lncRNA\_AF087999 (1/2-sbsRNA1) and the *SERPINE1* or *FLJ21870* mRNA 3' UTR, between lncRNA\_BC058830 (1/2-sbsRNA2) and the *CDCP1* mRNA 3' UTR, and between lncRNA\_AF075069 (1/2-sbsRNA3) or lncRNA\_BC009800 (1/2-sbsRNA4) and the *MTAP* or *FLJ21870* mRNA 3' UTR. Potential duplexes were fixed using the region that was predicted to be the most stably and perfectly base-paired and then expanded in both directions, allowing bulges or loops of up to 10 nucleotides, until base-pairing was no longer predicted. Briefly, *RNA\_RNA\_anneal* uses a recursive algorithm that predicts the most stable base pairs and their folding free-energy change ( $\Delta G$ ) based on thermodynamic data<sup>19,20</sup> that were extracted from the program RNAstructure 4.6 (<http://rna.urmc.rochester.edu/rnastructure.html>). Duplexes between other ncRNAs and mRNA 3' UTRs were likewise predicted using this approach. All data from *RNA\_RNA\_anneal* were validated using the program RNAstructure 4.6, which also provides  $\Delta G$  values.

Notably, to follow up our finding that ~13% of the ~1.6% of HeLa-cell protein-coding transcripts that are upregulated at least 1.8-fold on STAU1 downregulation<sup>1,2</sup> contain a single Alu element, a random resampling of 1.6% of total-cell mRNAs (NCBI RefSeq) 10,000 times showed that the presence of one or more Alu elements in the 3' UTRs of potential SMD targets (Supplementary Table 1) was enriched ~3.58-fold ( $P < 0.001$ ).

Perl program codes are available for downloading from [http://dbb.urmc.rochester.edu/labs/maquat/maquat\\_lab.htm](http://dbb.urmc.rochester.edu/labs/maquat/maquat_lab.htm).

**Plasmid constructions.** To construct pcDNA3.1/Zeo(+)-Chr11\_66193000–66191383, HeLa-cell genomic DNA was purified using DNeasy Blood & Tissue Kit (Qiagen) and amplified by PCR using the primer pair 5'-GATGCTCGAGTGGCATTGGCTTTACCACCTATG-3' (sense) and 5'-GTCAGGATCCTGCCTCAAGTCAAAGCACAACCTG-3' (antisense), where the underlined nucleotides specify a XhoI or BamHI site, respectively. The resultant PCR product was cleaved with XhoI and BamHI and inserted into XhoI- and BamHI-cleaved pcDNA3.1/Zeo(+) vector (Invitrogen).

To generate p1/2-sbsRNA1(S) or p1/2-sbsRNA1(S)-MS2bs, pcDNA3.1/Zeo(+)-Chr11\_66193000–66191383 was amplified using the primer pair 5'-GAGTCAAAGCTTAAAGGAGAGACAGTCTCACTCTG-3' (sense) and 5'-GTCAGCGGCCCGCAGTTGTAAGCATATTTGGGTTAC-3' (antisense) or 5'-GTCAGGATCCAGTTGTAAGCATATTTGGGTTAC-3' (antisense), respectively, where underlined nucleotides denote a HindIII, NotI or BamHI site, respectively. The resultant PCR products were cleaved with HindIII and either NotI or BamHI, respectively, and inserted into HindIII- and NotI-cleaved or HindIII- and BamHI-cleaved pcDNA3-MS2bs<sup>14</sup>.

Overlap extension PCR was used to construct p1/2-sbsRNA1(S)<sup>R</sup>. Two rounds of site-directed mutagenesis were performed using p1/2-sbsRNA1(S) and the following primer pairs: first round, 5'-GATATTCATTACTAACCCTGAACCCATACAGTTCAGCTTACCCTACAGTACTTCT-3' (sense) and 5'-AGAA GTACTGTAGTGGTAAAGCTGAACCTGATGGGTTTCAGGGTTAGTAATGATATC-3' (antisense); and second round, 5'-CCTGAACCCATACAGTTCAGCTCAGAACTACAGTACTTCTGTAGT-3' (sense) and 5'-ACTACAGAAGTACTGTAGTTCAGTGAACCTGATGGGTTTCAGG-3' (antisense), where mutagenic nucleotides are underlined.

To generate pFLUC-MS2bs, pFLUC<sup>13</sup> was amplified by PCR using the primer pair 5'-GAGTCAAAGCTTATGGAAGACGCCAAAAACATAAAGAAAGGC-3' (sense) and 5'-GTCAGGATCCTTACAATTGGACTTTCGCCCTTCTTG GC-3' (antisense), where underlined nucleotides specify a HindIII or BamHI site. The resultant PCR product was digested with HindIII and BamHI and inserted into HindIII- and BamHI-cleaved pcDNA3-MS2bs.

To construct pFlag-MS2-hMGFP, pMS2-HA<sup>13</sup> was amplified using the primer pair 5'-GATGGCTAGCCGCATGGACTACAAAGACGATGACGACAAGG GATCCGCTTACTACTTTACTCAGTTCG-3' (sense) and 5'-GTCAGATATC GTAGATGCCGGAGTTTGTCTGCG-3' (antisense), where underlined nucleotides specify an NheI or EcoRV site. The resultant PCR product was digested using NheI and EcoRV and inserted into NheI- and EcoRV-cleaved pMGFP vector (Promega).

To create p1/2-sbsRNA1(S)-hMGFP, pMGFP was amplified using the primer pair 5'-GATGCCTAGGGCGGTGATCAAGCCCGACATG-3' (sense) and 5'-GTCACTAGGGCCGCGCTGGCGGGGTAGTCC-3' (antisense), where underlined nucleotides identify the AvrII site. The resultant PCR product was digested with AvrII and inserted into the AvrII site of p1/2-sbsRNA1(S).

To construct pFLUC-FLJ21870 3' UTR, two fragments of the *FLJ21870* mRNA 3' UTR were amplified using HeLa-cell genomic DNA and the primer pairs 5'-GATGCTAGAGTGATCAACTTCGCCAACAAACACCAG-3' (sense) and 5'-CAGAAGGCTAGCCCGAAGAGAAC-3' (antisense), and 5'-CTCTTCGG GCTAGCCTTCTGG-3' (sense) and 5'-GTCAGGGCCCGAGACAGAGTCTC CGTTGCC-3' (antisense), where underlined nucleotides denote an XbaI, NheI, NheI or ApaI site, respectively. The resultant PCR fragments were digested using NheI and either XbaI or ApaI, and inserted simultaneously into pFLUC-SERPINE1 3' UTR<sup>5</sup> that had been digested with XbaI and ApaI.

To create pFLUC-SERPINE1 3' UTR  $\Delta$ (1/2-sbsRNA1-BS), two regions of the *SERPINE1* mRNA 3' UTR were amplified using pFLUC-SERPINE1 3' UTR and the primer pairs 5'-GAGTCAAAGCTTGGCATTCCGGTACTGTTGG-3' (sense) and 5'-CATCCATCTTTGTGCCCTACC-3' (antisense), and 5'-TCTTTAAA AATATATATATTTTAAATATAC-3' (sense) and 5'-TAGAAGGCACAGTCG AGG-3' (antisense), where underlined nucleotides denote a HindIII site. The resultant PCR fragments were phosphorylated using T4 polynucleotide kinase, digested with HindIII or ApaI (which binds upstream of where the antisense primer anneals), respectively, and inserted simultaneously into pFLUC-SERPINE1 3' UTR that had been digested with HindIII and ApaI.

To generate pFLUC-SERPINE1 1/2-sbsRNA1-BS, 1/2-sbsRNA1-BS was amplified using pFLUC-SERPINE1 3' UTR and the primer pair 5'-GATGTTTA AATAATGCACCTTTGGGAGGCCAAGG-3' (sense) and 5'-GATGTTTAAAG ACGGGGCTCTGGTATGTTC-3' (antisense), where underlined nucleotides denote a DraI site. The resultant PCR product was then digested with DraI. Meanwhile, pFLUC-No SBS was digested with HindIII and ApaI, and the released FLUC-No SBS region was subsequently digested with DraI. All three fragments from the pFLUC-No SBS digestions were then ligated to the PCR product.

To generate pTRE-FLUC-SERPINE1 3' UTR or pTRE-FLUC-FLJ21870 3' UTR, pFLUC-SERPINE1 3' UTR was amplified using the primer pair 5'-GATACCGCGGATGGAAGACGCCAAAAACATAAAG-3' (sense) and 5'-GTCAGAATTCGCTTCTATTAGATTACATTCATTTCAC-3' (antisense), or pFLUC-FLJ21870 3' UTR was amplified using the primer pair 5'-GATACC GCGGATGGAAGACGCCAAAAACATAAAG-3' (sense) and 5'-GTCAGAAT TCGAGACAGAGTCTCCGTTGCC-3' (antisense), where underlined nucleotides denote a SacII or EcoRI site, respectively in each primer pair. The resultant PCR product was digested with SacII and EcoRI and inserted into SacII- and EcoRI-cleaved pTRE vector (Clontech).

**Cell culture, transient transfection and formaldehyde crosslinking.** Human (HeLa or HaCaT) cells ( $2 \times 10^6$  per 60-mm dish or  $7.5 \times 10^7$  per 150-mm dish) were grown in the medium DMEM (GIBCO) containing 10% FBS (GIBCO). Cells were transiently transfected with the specified plasmids by using Lipofectamine 2000 Transfection Reagent (Invitrogen) or with the specified siRNA by using Oligofectamine Transfection Reagent (Invitrogen) as previously described<sup>1</sup>. The siRNAs used were *STAU1*-directed siRNA<sup>13</sup>, 1/2-sbsRNA1-directed siRNA (5'-CCUGUACCCUUCAGCUUACdTdT-3'), 1/2-sbsRNA1(A)-directed siRNA (5'-AUGACUUUGGGCAAAGUACdTdT-3'), *DICER1*-directed siRNA (Ambion), *AGO2*-directed siRNA (Ambion), *SERPINE1*-directed siRNA (Ambion), *FLJ21870*-directed siRNA (Ambion), *RAB11FIP1*-directed siRNA (Ambion), 1/2-sbsRNA2-directed siRNA (5'-GGUGCAAAGACAGCAUCCdTdT-3'), 1/2-sbsRNA3-directed siRNA (5'-UAGUAGUCAAGACCAAUUCUAdTdT-3'), 1/2-sbsRNA4-directed siRNA (5'-UGGCAUCCAGUUGAGUUUdTdT-3') and a nonspecific siRNA, *Silencer* Negative Control #1 siRNA (Ambion). Notably, all lncRNA-directed siRNAs used in this study target a sequence outside the Alu element. For all immunoprecipitations, cells were crosslinked using 1% formaldehyde for 10 min at 25°C and subsequently quenched with 0.25 M glycine for 5 min at room temperature before lysis<sup>1</sup>. In experiments that blocked protein synthesis, cells were incubated with 300  $\mu\text{g ml}^{-1}$  cycloheximide (Sigma) 3 h before lysis.

For mRNA half-life measurements, Tet-Off HeLa cells (Clontech) were transfected with the specified siRNA in the presence of 2  $\mu\text{g ml}^{-1}$  doxycycline (Clontech). After 48 h, the medium was replaced to remove doxycycline, and cells were transfected with the indicated reporter and reference plasmids. After 4 h, an aliquot of cells was collected. Then, 2  $\mu\text{g ml}^{-1}$  doxycycline was added to the remaining cells to silence reporter gene transcription, and aliquots of cells were collected at time points thereafter.

Scrape-injury repair assays were essentially performed as previously published<sup>21,22</sup>. Briefly, 2 days after transfection with siRNA, monolayer cultures of HaCaT cells at 90% confluence in 100-mm dishes were scratched in nine places using a P200 pipette tip (VWR) and uniform pressure to create denuded areas that were 0.9 mm wide. Cells were washed once with growth medium (DMEM supplemented with 10% FBS), which removes scratch-generated debris and generates smooth wound edges, and then cultured for an additional 16 h with monitoring.

**Protein purification, immunoprecipitation and western blotting.** HeLa cells were lysed, and protein was isolated using hypotonic buffer consisting of 10 mM Tris-Cl (pH 7.4), 150 mM NaCl, 2 mM EDTA, 0.5% Triton X-100, 2 mM benzamide,

1 mM phenylmethylsulphonyl fluoride and 1 tablet complete protease inhibitor cocktail in 50 ml (Roche). If the cells had been formaldehyde crosslinked, they were sonicated six times for 30 s to facilitate lysis. Immunoprecipitation was performed as previously described<sup>1</sup>. In experiments that involved formaldehyde crosslinking, crosslinks were reversed by heating at 65 °C for 45 min after immunoprecipitation. Western blotting was performed as previously described<sup>1</sup>. Antibodies consisted of anti-STAU1 (ref. 23), anti-calnexin (Calbiochem), anti-Flag (Sigma), anti-ILF3 (Santa Cruz Biotechnology), anti-FMRI (Santa Cruz Biotechnology), anti-HA (Roche), anti-DICER1 (Santa Cruz Biotechnology), anti-AGO2 (Santa Cruz Biotechnology) and anti-BAG5 (Abcam) antibodies.

**RNA purification, poly(A)<sup>+</sup> RNA preparation and RT coupled to either semi-quantitative or quantitative real-time PCR.** RNA was purified from total, nuclear or cytoplasmic HeLa-cell fractions or immunoprecipitated from total-cell lysates using TRIzol (Invitrogen) as previously described<sup>1</sup>. Poly(A)<sup>+</sup> RNA was extracted from total-cell RNA by using the Oligotex mRNA Mini Kit (Qiagen). Alternatively, RNA derived from different human tissues was obtained from Ambion. Semiquantitative RT-PCR and quantitative real-time RT-PCR were performed as previously described<sup>1</sup>, using the designated primer pairs (Supplementary Table 4). In Supplementary Fig. 2c, RT was primed using oligo(dT)<sub>18</sub> rather than random hexamers. Semiquantitative RT-PCR analyses situated under the wedges in the leftmost lanes of figures involved twofold dilutions of RNA and show that the data fall within the linear range. RT-PCR values plotted as histograms include the standard deviation obtained in the specified number of independently performed experiments.

**RNase protection assay and primer extension.** For the RNase protection assay, the RPA III Ribonuclease Protection Assay Kit (Ambion) was used. Uniformly

labelled RNA probes (10<sup>7</sup> c.p.m. µg<sup>-1</sup>) were generated by transcribing linearized pcDNA3.1/Zeo(+)\_Chr11\_66193000–66191383 (which contains 1/2-sbsRNA1(S) and upstream and downstream flanking sequences) *in vitro* using [ $\alpha$ -<sup>32</sup>P]UTP (PerkinElmer) and the MAXIscript Kit (Ambion). Each probe (10<sup>5</sup> c.p.m.) was incubated with poly(A)<sup>+</sup> HeLa-cell RNA (10 µg) or yeast RNA (10 µg) in hybridization buffer (Ambion) at 42 °C for 12 h and subsequently cleaved using RNase A and RNase T1 (1/200; Ambion) at 37 °C for 30 min. Input probe (1/1000) and cleaved products were resolved in a 3.5% denaturing polyacrylamide gel and visualized using a Typhoon PhosphorImager (GE Healthcare).

Primer extension was performed using poly(A)<sup>+</sup> HeLa-cell RNA (10 µg), SuperScript II reverse transcriptase (Invitrogen) and the 1/2-sbsRNA1-specific antisense primer 5'-GAGTTAAAAGAGGCTGCAGTG-3'. DNA sequencing was executed using the SILVER SEQUENCE DNA Sequencing System (Promega), the same antisense primer and pcDNA3.1/Zeo(+)\_Chr11\_66193000–66191383. Primer extension and sequencing products were resolved in an 8% denaturing polyacrylamide gel and visualized using a Typhoon PhosphorImager.

**Fluorescence and phase contrast microscopy.** Cells were visualized using an Eclipse TE2000-U inverted fluorescence microscope (Nikon), and a 480-nm excitation wavelength was used for phase contrast microscopy. Images were captured using TILLvisION software (TILL Photonics).

- Marion, R. M., Fortes, P., Beloso, A., Dotti, C. & Ortin, J. A human sequence homologue of Staufien is an RNA-binding protein that is associated with polysomes and localizes to the rough endoplasmic reticulum. *Mol. Cell. Biol.* **19**, 2212–2219 (1999).